Applied Physics Letters

Wideband detection of electromagnetic signals by high-T_c Josephson junctions with comparable Josephson and thermal energies

Cite as: Appl. Phys. Lett. **116**, 082601 (2020); https://doi.org/10.1063/1.5142400
Submitted: 12 December 2019 . Accepted: 12 February 2020 . Published Online: 25 February 2020

V. V. Pavlovskiy, I. I. Gundareva, O. Y. Volkov, and Y. Y. Divin

Applied Physics Letters ARTICLE scitation.org/journal/apl

Wideband detection of electromagnetic signals by high-T_c Josephson junctions with comparable Josephson and thermal energies

Cite as: Appl. Phys. Lett. **116**, 082601 (2020); doi: 10.1063/1.5142400
Submitted: 12 December 2019 · Accepted: 12 February 2020 ·
Published Online: 25 February 2020

V. V. Pavlovskiy,[1] I. I. Gundareva,[1,2] O. Y. Volkov,[1] and Y. Y. Divin[1,2,a)]

AFFILIATIONS

[1]Kotelnikov Institute of Radio Engineering and Electronics, Russian Academy of Sciences, 125009 Moscow, Russia
[2]Peter Grünberg Institute, Forschungszentrum Jülich, 52425 Jülich, Germany

[a)]**Author to whom correspondence should be addressed:** yyd@cplire.ru

ABSTRACT

Detection mechanisms in Josephson junctions with energies E_j comparable to thermal energies kT have been studied. The responses ΔV of $YBa_2Cu_3O_{7-x}$ bicrystal junctions to monochromatic radiation with frequencies f ranging from 94 GHz to 3.1 THz can be described in terms of classical rectification on a static nonlinear V–I curve at low frequencies and frequency modulation of the ac Josephson current at high frequencies, with an interplay between these mechanisms at intermediate frequencies. An electrical noise-equivalent power of $(9 \pm 3) \times 10^{-15}$ W/Hz$^{1/2}$, a responsivity of $(3.4 \pm 0.5) \times 10^5$ V/W, and a dynamic power range of 5×10^4 have been demonstrated for the square-law classical detection of 94 GHz radiation with the junctions at 50 K. The effect of background radiation on the V–I curves of $YBa_2Cu_3O_{7-x}$ bicrystal junctions was found to have an optical noise-equivalent temperature of $\lesssim$30 mK/Hz$^{1/2}$. The main contribution to the effect comes from the interplay between the classical and Josephson detection mechanisms. The spectral and power dependencies of the responses ΔV of Josephson junctions have been numerically simulated within the resistively shunted junction model at various values of kT/E_j, and the results are in acceptable agreement with the experimental data.

Conventional semiconductor detectors of electromagnetic radiation exhibit a decrease in efficiency when their operational frequencies are extended into the terahertz (THz) range.[1] Moreover, this operational extension of electronic and photonic detectors into the THz range often requires their cooling to very low temperatures, which affords the opportunity for superconductor detectors to compete with these earlier THz devices. However, the well-known superconductor–insulator–superconductor (SIS) detectors, which are based on the nonlinearity of quasiparticle currents in low-T_c SIS junctions,[1] operate effectively only up to the gap frequency of the superconductor, which is of approximately 700 GHz for low-T_c superconductor niobium (Nb).

Additional, but less studied, possibilities arise when using the strong dynamic nonlinearity of the ac Josephson current in high-T_c junctions. The detection of electromagnetic signals using the ac Josephson effect in superconducting tunnel junctions was first described in an original paper by Brian Josephson.[2] An applied signal with frequency f modulates the frequency of the ac Josephson supercurrent and, correspondingly, results in dc contributions to the supercurrent at dc voltages $V = nhf/2e$ ($n = 0, 1, 2, \ldots$).[2] At low signal levels, the suppression ΔI_c of the critical current I_c and the appearance of the first current step I_1 at $V = hf/2e$ are the main modifications of the dc V–I curve of the Josephson junction. In the first experiments with Nb–Nb point-contacts at 1.3 K,[3] a response proportional to ΔI_c has been observed up to 1 THz, and a noise-equivalent power (NEP) of 10^{-12} W/Hz$^{1/2}$ has been demonstrated at 75 GHz.

A more detailed analytical study of the Josephson detector has been carried out against the framework of the noise-free resistively shunted junction (RSJ) model.[4] A frequency-selective voltage response $\Delta V(V)$ with an odd-symmetric resonance at $V \cong hf/2e$ was found. The wideband Josephson response $\Delta V(V)$ at $V \ll hf/2e$ is proportional to the first derivative dV/dI of the V–I curve. It is due to the suppression ΔI_c and decreases with the frequency as $1/f^2$. The response $\Delta V(V)$ at $V \gg hf/2e$ is frequency-independent and proportional to the second derivative d^2V/dI^2 of the V–I curve, as in a classical rectifier. In the noise-free case, however, classical detection is found only at low f and high V, where the values of d^2V/dI^2 and the responses are small.

The effect of thermal noise on Josephson detection has been examined using numerical simulations.[5,6] The response ΔV and the NEP of Josephson detectors have been calculated for a few combinations of V, f, and the ratio $\gamma = E_j/kT$, where $E_j = hI_c/4\pi e$ is the Josephson energy and kT is the thermal energy.[5,6] Recently, an extended set of characteristics, including the power and spectral ranges of detectors, have been calculated numerically at various γ and analytically at $\gamma \geq 1$.[7] In the case of $\gamma \sim 1$, thermal noise plays a unique role, extending the nonlinear Josephson dynamics to a wide frequency range up to the characteristic Josephson frequency $f_c = 2eI_cR_n/h$ (R_n is the junction resistance) and at the same time maintaining a pronounced nonlinearity of the dc V–I curve. It is intuitively clear that classical rectification in this case can be observed in a wider frequency range, at $f < f_c$, than in that of the case[4] without noise.

Classical detection has been observed in Nb–Nb Josephson junctions at frequencies up to 150 GHz[8] and 290 GHz,[9] which have been scaled with the characteristic frequencies f_c of the utilized junctions. Thus, there is the possibility of extending the operation of classical detection to higher frequencies and/or increasing its temperature range using high-T_c Josephson junctions. To date, however, detection has been studied in low-resistance high-T_c junctions,[10–15] where interest has been concentrated mainly on frequency-selective Josephson detection, and only a few data are available[12,15] for wideband Josephson detection with an electrical NEP of 3×10^{-13} W/Hz$^{1/2}$ and an optical noise-equivalent temperature (NET) of 1 K/Hz$^{1/2}$. Classical detection in high-T_c junctions has not received due attention. Here, we present our experimental results on wideband detection using high-resistance high-T_c junctions with Josephson energies comparable to thermal energies.

[001]-Tilted $YBa_2Cu_3O_{7-x}$ (YBCO) bicrystal junctions have been fabricated by the epitaxial growth of $YBa_2Cu_3O_{7-x}$ thin films on (110) $NdGaO_3$ bicrystal substrates with misorientation angles of $2 \times 11.3°$ and $2 \times 14°$.[16] Narrow $YBa_2Cu_3O_{7-x}$ bridges [Fig. 1(a)] crossing a bicrystal boundary [dashed line in Fig. 1(a)] are patterned by UV photolithography and wet etching. Log-periodic sinuous Au antennas integrated with the bicrystal junctions [Fig. 1(b)] are fabricated by a lift-off procedure. A selected junction with a silicon (Si) hyperhemispheric lens is mounted in a vacuum chamber in either an optical cryostat, where liquid nitrogen is at low pressure, or a Stirling cooler, which is magnetically shielded by mu-metal.[10] The junctions are current-biased with large output resistances $R \gg R_n$. Immunity to electrical interferences is enhanced by using symmetrical circuitry in current-bias electronics, with a virtual ground for both a current supply and a differential preamplifier, as is done in voltage-bias electronics for low-resistance Josephson junctions.[14] The external electronics are connected to the junction electronics via feedthrough filters. At operational temperatures T above 48 K, these measures are sufficient to work in a situation where the main noise in the junction is due to intrinsic thermal noise with an effective noise current of $I_n = 8\pi ekT/h$.

Gunn oscillators, frequency multipliers, and an optically pumped CH_3OH laser are used as signal sources with frequencies f from 0.094 to 3.1 THz. The radiation from a 94 GHz Gunn oscillator is fed through fixed (up to 60 dB) and variable (up to 50 dB) waveguide attenuators to a scalar horn and then to a parabolic mirror. Frequency multipliers (×2, ×3, and ×5) are driven by a Gunn oscillator and operate in the same optical arrangement. After passing a switchable set of quasi-optical absorbers (0–50 dB), radiation from the Gunn oscillator or multipliers is focused on the junction by a second parabolic mirror. The output power of the laser is attenuated by a set of quasi-optical absorbers. These sets of waveguide attenuators and quasi-optical absorbers are adequate to guarantee the power levels, which are inside the dynamic range of the square-law Josephson detector and are required for the comparison of the response mechanisms for frequencies from 94 GHz to 3.1 THz.

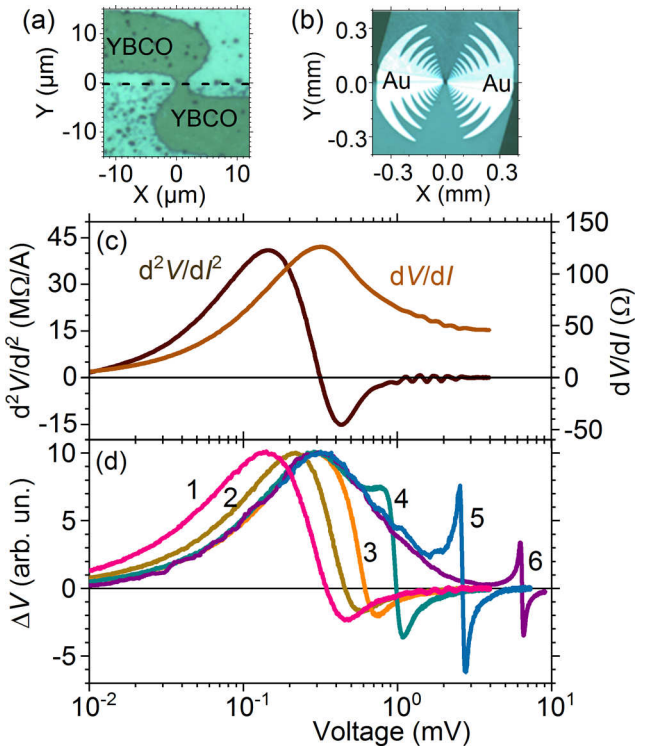

FIG. 1. (a) Microphotograph of a $YBa_2Cu_3O_{7-x}$ (YBCO) bicrystal junction, where the dashed line indicates a bicrystal boundary. (b) Microphotograph of an integrated Au antenna. (c) First (dV/dI) and second (d^2V/dI^2) derivatives of the dc V–I curve for a typical junction with $R_n = 46\,\Omega$ at 50 K. (d) Voltage responses $\Delta V(V)$ of the same junction to radiation with frequencies (THz) as follows: 1—0.094, 2—0.188, 3—0.282, 4—0.47, 5—1.287, and 6—3.106.

Figure 1(c) shows the first and second derivatives of the V–I curve vs voltages V for a typical bicrystal junction with $R_n = 46\,\Omega$ and $I_cR_n = 1.0$ mV at $T = 50$ K. The maximum value of $(dV/dI)_{max}$ is equal to 126 Ω at a voltage $V_{1max} = 0.32$ mV, while the maximum value of d^2V/dI^2 is equal to 41 MΩ/A at a voltage $V_{2max} = 0.14$ mV. An oscillatory pattern in the voltage dependencies of the derivatives at 0.8 mV $< V <$ 3.5 mV reflects the frequency-selective shunting of Josephson oscillations by multiple antenna resonances and is described in detail elsewhere.[17]

The voltage responses $\Delta V(V)$ of the same junction to monochromatic radiation with frequencies from 0.094 to 3.1 THz are presented in Fig. 1(d). The response $\Delta V(V)$ for $f = 0.094$ THz (curve 1) reaches a maximum at voltage V_{max}, which is equal to the voltage V_{2max} [Fig. 1(c)]. The response $\Delta V(V)$ changes the sign at voltage V_0, and its form is reminiscent of the dependence of d^2V/dI^2 vs V [Fig. 1(c)], which is a reason for considering this response $\Delta V(V)$, at least at low

voltages $V < V_0$, as the result of classical rectification. There is a noticeable 30 μV shift in the voltage V_0 relative to a similar voltage in the dependence d^2V/dI^2 vs V. The shifts in voltage V_0 increase even more in the responses $\Delta V(V)$ at higher frequencies f of 0.188 THz (curve 2), 0.284 THz (curve 3), and 0.470 THz (curve 4). However, the values of V_0 are still above the values of $hf/2e$, which are expected for the locking of Josephson oscillations with external signals. Also, the maxima of $\Delta V(V)$ (curves 2–4) shift to higher voltages, until the V_{max} value for curve 4 [Fig. 1(d)] reaches the V_{1max} value of the maximum dV/dI [Fig. 1(c)]. With further increases in frequency to 1.287 THz (curve 5) and 3.106 THz (curve 6), the responses $\Delta V(V)$ begin to possess all the attributes of the Josephson response. They are proportional to dV/dI vs V at $V < 1$ mV and demonstrate odd-symmetric resonances at $V = hf/2e$. Thus, with the increase in signal frequency, the detection mechanism varies from a classical mode, i.e., rectification on a nonlinear dc V–I curve, to a Josephson mode characterized by suppression ΔI_c at low voltages and locking of Josephson oscillations by the external signal.

A comparison of the responses $\Delta V(V)$ of $YBa_2Cu_3O_{7-x}$ bicrystal junctions with various parameters R_n, I_c, and γ at various frequencies f requires either the values of the ac currents I_ω induced by the signals or a self-calibration procedure. To realize the latter case, the ratios of the responses ΔV_2, measured at the dc voltage bias V_{2max}, and ΔV_1, measured at the dc voltage bias V_{1max}, are needed to clarify the types of responses. Numerical simulations of the spectral responses $\Delta V_2(f)$ and $\Delta V_1(f)$ have been carried out using the Smoluchowski equation for RSJ-like junctions with thermal noise,[6] namely

$$\omega_c^{-1}\frac{\partial\sigma}{\partial t}+\frac{\partial}{\partial\varphi}\left[f(\varphi)\sigma\right]=\gamma\frac{\partial^2\sigma}{\partial\varphi^2}, \quad (1)$$

where $\sigma(t, \varphi)$ is the probability density of finding the phase φ at time t at the junction, $\omega_c = 2\pi f_c$, $f(\varphi, t) = i - \sin\varphi$, $i = I/I_c$ is the normalized current through the junction, and $\gamma = 4\pi ekT/hI_c$. The effect of electromagnetic radiation with frequency ω on the junction is taken into account by adding an induced current $i_\omega \sin\omega t$ to $f(\varphi, t)$ with a normalized amplitude $i_\omega = I_\omega/I_c$.

Figure 2(a) shows the results for γ values ranging from 0.005 to 2. The responses $\Delta V_2(f)$ (solid lines) have a frequency-independent part and decrease as $1/f^2$. The 3 dB decreases in the responses take place at frequencies ranging from 0.22 to 1.8 for junctions with γ values ranging from 0.005 to 2. The spectral response $\Delta V_1(f)$ (dots) increases proportionally to f^2, reaches a maximum at a frequency $f_m(\gamma)$, decreases as $1/f^2$ at higher frequencies, and shows responses approximately twice as high as those of $\Delta V_2(f) \propto 1/f^2$ at the same frequencies. The f_m values vary from 0.23 to 4.1 in a wide range of γ values from 0.005 to 2. The maxima of the responses ΔV_2 are always higher than those of the responses ΔV_1, while the bandwidths Δf of both responses are comparable.

The calculated ratios $\Delta V_2(f)/\Delta V_1(f)$ are shown in Fig. 2(b) by dashed lines for the γ values of 0.02 and 0.5. The experimental data are taken from the responses of four junctions with resistances R_n ranging from 6 to 96 Ω at the temperatures of 50 K (filled symbols), 78 K (open circles), and 83 K (open diamonds) to the signals with frequencies ranging from 0.094 to 3.106 THz. The experimental data are for γ values ranging from 0.01 to 0.6. The measured and calculated $\Delta V_2(f)/\Delta V_1(f)$ follow the same pattern: a frequency-independent part at $f/f_c > 2$ and a rapid rise at low frequencies, with a threshold that is

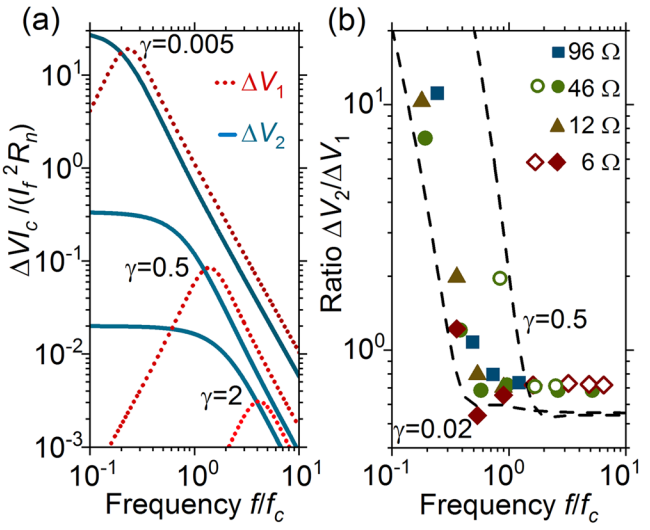

FIG. 2. (a) Simulated spectral responses $\Delta V_1(f)$ (dots) and $\Delta V_2(f)$ (solid lines) for various values of γ for two current biases on Josephson junctions, where dV/dI and d^2V/dI^2 have their maxima, correspondingly. (b) Ratio of the spectral responses $\Delta V_2(f)/\Delta V_1(f)$ measured for $YBa_2Cu_3O_{7-x}$ bicrystal junctions with R_n from 6 to 96 Ω at 50 K (filled symbols), 78 K (open circles), and 83 K (open diamonds). The dashed lines are the ratios $\Delta V_2(f)/\Delta V_1(f)$ obtained from the simulated data $\Delta V(f)$ for $\gamma = 0.02$ and 0.5.

dependent on γ. For a $\Delta V_2(f)/\Delta V_1(f)$ ratio less than 1, the response $\Delta V(V)$ at these frequencies is described by Josephson detection. For a $\Delta V_2(f)/\Delta V_1(f)$ ratio greater than 1, the response $\Delta V(V)$ is described by an interplay between the classical and Josephson detection mechanisms, becoming purely classical only at low frequencies.

Figure 3(a) shows the electrical characteristics of the $YBa_2Cu_3O_{7-x}$ bicrystal junction with $R_n = 96\,\Omega$ at 50 K. The V–I curve for currents between 5 and 10 μA demonstrates highly nonlinear behavior, which is reflected in the maximum values of the derivatives: $(dV/dI)_{max} = 188\,\Omega$ and $(d^2V/dI^2)_{max} = 94\,M\Omega/A$. The best fit of the simulated V–I curves to the experimental ones is found for $\gamma = 0.1$ [dashed line in Fig. 3(a)]. The junction demonstrates a similar modification of the responses ΔV to radiation with various frequencies, as in Fig. 1, but with better sensitivity to radiation for frequencies up to 0.47 THz.

Figure 3(b) shows the dependence of the response ΔV vs attenuation of incident 94 GHz radiation, when the junction is biased at a current of 7 μA corresponding to the maximum of d^2V/dI^2. The power of the incident 94 GHz radiation is attenuated to levels as low as −71 dB with an accuracy of 1 dB. The measured response ΔV [filled squares, Fig. 3(b)] increases from 0.35 to 0.55 mV at an attenuation from −10 to −21 dB, reaches a maximum, and decreases approximately as $P^{1/2}$, and then, at an attenuation of less than −37 dB, $\Delta V \propto P$.

Several dependencies of ΔV vs absorbed power P_a have been numerically simulated for γ values ranging from 0.01 to 2. The absorbed power P_a has been calculated as $P_a = I_f^2 ReZ/2$, where Z is the junction impedance and ReZ is equal to the differential resistance dV/dI at low frequencies f.[6] A dashed line in Fig. 3(b) represents the calculated response ΔV vs the absorbed power $I_f^2(dV/dI)/2$ (upper scale), which shows the best fit to the experimental data $\Delta V(P)$. The value of

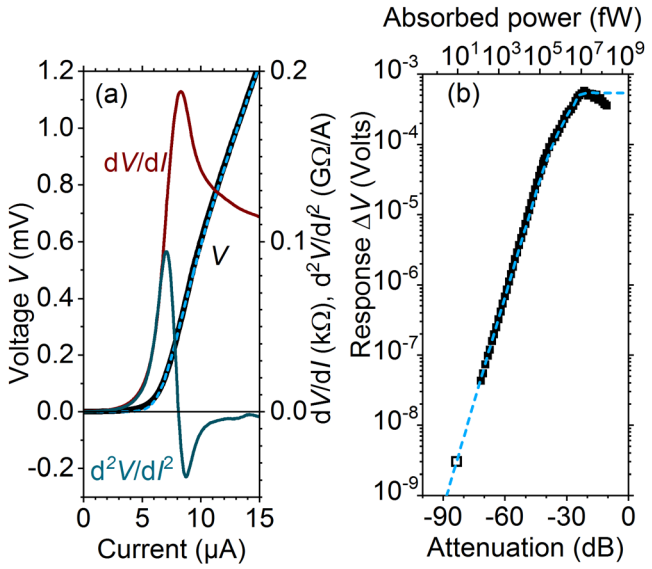

FIG. 3. (a) Electrical characteristics of a $YBa_2Cu_3O_{7-x}$ bicrystal junction with $R_n = 96\,\Omega$ at 50 K. The dashed line is the calculated *V–I* curve for $\gamma = 0.1$. (b) Response ΔV (filled squares) of the junction vs attenuation of 94 GHz radiation. The junction is biased at the maximum of d^2V/dI^2. The dashed line is the calculated response ΔV vs absorbed power (upper scale) for $\gamma = 0.1$. The open square is the response equal to the measured voltage noise V_n at 1 Hz bandwidth.

$\gamma = 0.1$ used for the best fit to the experimental $\Delta V(P)$ data is the same as the corresponding value for the best fit of the *V–I* curve [Fig. 3(a)]. The fit is very good at attenuation levels from −71 to −21 dB. Thus, we can ascribe the calculated absorbed power (upper scale) to the attenuation levels in the experimental data and obtain a value for the responsivity $r = \Delta V/P$ of $(3.4 \pm 0.5) \times 10^5$ V/W from the data in Fig. 3(b). This value is in agreement with the classical responsivity $r = (d^2V/dI^2)/2(dV/dI) = (3.9 \pm 0.2) \times 10^5$ V/W calculated from the experimental data in Fig. 3(a). This proves the correctness of the assignment of the upper power scale to the attenuation levels at the lower scale in Fig. 3(b).

An open square in Fig. 3(b) represents a response equal to the measured voltage noise $V_n = 3 \times 10^{-9}$ V of the junction in the 1 Hz bandwidth, when the junction is biased at the maximum of d^2V/dI^2. It is placed in the ΔV–P plot on the intersection of the fitting curve with the experimental data, which has a linear dependence $\Delta V \propto P$ at low power levels. Thus, the position of the open square on the power scale gives the value of the NEP equal to $(9 \pm 3) \times 10^{-15}$ W/Hz$^{1/2}$. According to the definitions,[18] this NEP belongs to the electrical NEP. As follows from Fig. 3(b), a dynamic power range between the NEP value and the maximum power value, where the response $\Delta V(P)$ deviates from the linear dependence by less than 1 dB, is equal to 47 ± 1 dB. The obtained NEP value for classical detection is much better than the NEP values of approximately 3×10^{-13} W/Hz$^{1/2}$ demonstrated earlier[12] for Josephson detection with high-T_c junctions at 50 K.

It is found that the *V–I* curves of our high-T_c bicrystal junctions are very sensitive to background radiation, and this effect is demonstrated in Fig. 4 for the junction with $R_n = 96\,\Omega$ at 50 K. The polyethylene window of the cryostat is first closed by an Eccosorb absorber and then by an Au-coated metal plate. This results in a sharpening of the derivatives, accompanied by a 12% increase in the maximum of d^2V/dI^2 and a 7% increase in the maximum of dV/dI. The absorber might be considered as a source of blackbody radiation with a temperature of 300 K, while the Au-coated plate has much lower emissivity.

The change in background illumination results in the response $\Delta V(I)$ shown in Fig. 4, which is calculated by the integration of the difference between the two dependencies dV/dI vs I measured for high (dashed line) and low (solid line) levels of background radiation. The response $\Delta V(I)$ has a bell shape, with a maximum at a current of 7.5 μA, which is located between the currents, where dV/dI and d^2V/dI^2 have their maxima. These circumstances allow us to consider the response $\Delta V(I)$ to broadband background radiation as a result of the interplay of the Josephson ($\propto dV/dI$) and classical ($\propto d^2V/dI^2$) detection modes, rather than of one of these limiting cases.

A maximum value of 28 μV is found for the response $\Delta V(I)$ due to background radiation. Adopting a conservative estimate for the difference in effective temperatures of $\Delta T \leq 300$ K for the data in Fig. 4, the temperature responsivity $\Delta V/\Delta T$ can be estimated as $\Delta V/\Delta T \geq 0.1\,\mu$V/K. The noise-equivalent temperature (NET) is less than 0.03 K/Hz$^{1/2}$ if we use the measured value of the voltage noise $V_n = 3 \times 10^{-9}$ V/Hz$^{1/2}$. The value of the optical NET ≤ 0.03 K/Hz$^{1/2}$, which is obtained for the interplay between the classical and Josephson detection modes, is much better than the NET values for low-resistance high-T_c junctions operating in the Josephson detection mode.[15]

In summary, we have studied the wideband detection of electromagnetic signals using high-resistance $YBa_2Cu_3O_{7-x}$ bicrystal junctions with Josephson energies E_j comparable to the thermal energy kT. In this case, thermal noise extends the nonlinear Josephson dynamics to a wide frequency range and, at the same time, retains a pronounced nonlinearity for the dc *V–I* curves. The responses ΔV of the junctions

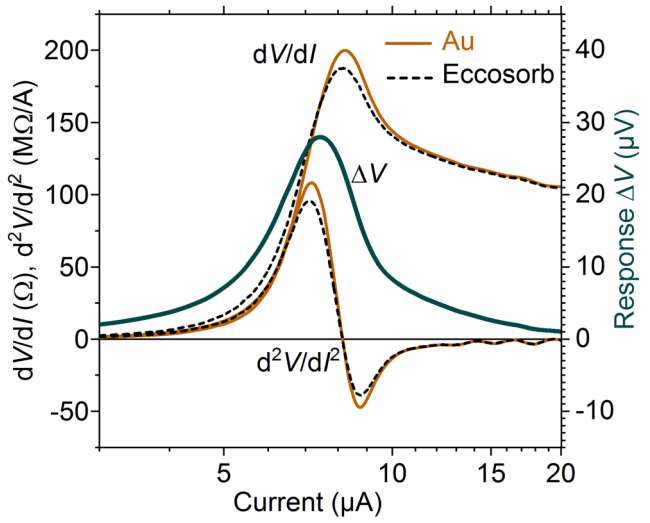

FIG. 4. Effect of background radiation on the *V–I* curve of the junction with $R_n = 96\,\Omega$ at 50 K. The derivatives are shown by solid lines, when an Au-coated metal plate is present on an optical input of the cryostat, and by dashed lines, when an Eccosorb absorber is present. The response $\Delta V(I)$ is obtained by the integration of the difference between the dV/dI vs I measured for two background levels.

to monochromatic radiation with frequencies f ranging from 94 GHz to 3.1 THz have been found to be described by the interplay of classical rectification and frequency modulation of the ac Josephson current. An electrical NEP of 9 fW/Hz$^{1/2}$ and an optical NET less than 30 mK/Hz$^{1/2}$ have been demonstrated for $YBa_2Cu_3O_{7-x}$ bicrystal junctions at 50 K, which are the best results obtained for wideband detection with high-T_c Josephson junctions. This work paves the way for extending highly efficient wideband detection with high-T_c Josephson junctions deep into the terahertz range.

The work was carried out within the framework of the state task of Russian Ministry of Science and High Education and partially was supported by the Russian Foundation for Basic Research, the project No.17-07-00779 A. Also, I.G. and Y.D. wish to thank Forschungszentrum Jülich for partial support.

REFERENCES

[1]A. Rogalski and F. Sizov, Opto-Electron. Rev. **19**, 346 (2011).
[2]B. D. Josephson, Phys. Lett. **1**, 251 (1962).
[3]C. C. Grimes, P. L. Richards, and S. Shapiro, J. Appl. Phys. **39**, 3905 (1968).
[4]H. Kanter and F. L. Vernon, J. Appl. Phys. **43**, 3174 (1972).
[5]A. N. Vystavkin, V. N. Gubankov, L. S. Kuzmin, K. K. Likharev, V. V. Migulin, and V. K. Semenov, Rev. Phys. Appl. **9**, 79 (1974).
[6]K. K. Likharev, *Dynamics of Josephson Junctions and Circuits* (Gordon and Breach, New York, USA, 1986).
[7]V. V. Pavlovskiy and Y. Y. Divin, J. Commun. Technol. Electron. **64**, 1003 (2019).
[8]H. Tolner, J. Appl. Phys. **48**, 691 (1977).
[9]Y. Y. Divin, A. D. Malov, and F. Y. Nad', Radiotekh. Elektron. **23**, 1875 (1978).
[10]Y. Y. Divin, U. Poppe, O. Y. Volkov, and V. V. Pavlovskii, Appl. Phys. Lett. **76**, 2826 (2000).
[11]W. W. Xu, J. Chen, L. Kang, and P. H. Wu, Sci. China Technol. Sci. **53**, 1247 (2010).
[12]J. Du, K. Smart, L. Li, K. E. Leslie, S. M. Hanham, D. H. C. Wang, C. P. Foley, F. Ji, X. D. Li, and D. Z. Zeng, Supercond. Sci. Technol. **28**, 084001 (2015).
[13]A. Sharafiev, M. Malnou, C. Feuillet-Palma, C. Ulysse, P. Febvre, J. Lesueur, and N. Bergeal, Supercond. Sci. Technol. **29**, 074001 (2016).
[14]A. V. Snezhko, I. I. Gundareva, M. V. Lyatti, O. Y. Volkov, V. V. Pavlovskiy, U. Poppe, and Y. Y. Divin, Supercond. Sci. Technol. **30**, 044001 (2017).
[15]M. Tarasov, E. Stepantsov, A. Kalabukhov, M. Kupriyanov, and D. Winkler, JETP Lett. **86**, 718 (2008).
[16]Y. Y. Divin, U. Poppe, I. M. Kotelyanskii, V. N. Gubankov, and K. Urban, J. Commun. Technol. Electron. **53**, 1137 (2008).
[17]V. V. Pavlovskii, I. I. Gundareva, O. Y. Volkov, Y. Y. Divin, and V. N. Gubankov, J. Commun. Technol. Electron. **58**, 951 (2013).
[18]See http://www.iram.fr/~leclercq/Reports/About_NEP_photon_noise.pdf for information about the definitions of the electrical and/or optical noise equivalent power NEP (last accessed December 04, 2019).